Optica Applicata VIII/2, 1978

*Andrzej Romanowski**

Coma and anticoma of deflecting-focusing unit in scanning microscope

Deflection coma and anticoma in the scanning microscope has been discussed. The influence of saddle dimensions of the deflecting coils as well as the sizes of the deflecting-focusing unit have been take into consideration. The results obtained have been verified experimentally.

1. Introduction

The deflection coma and anticoma of a deflecting-focusing units [1] are introduced by a deflecting doublet (DD) and the end lens. Deviation $\Delta x, \Delta y$ evoked by deflection coma and anticoma depends upon the deflection γ_x, γ_y of the beam in DD [1], the aperture angle ω, and the deflection errors in the deflecting units.

The coefficients of deflection coma and anticoma of DD (for identical vertical and horizontal coils) have the form [2]:

$$[0020]_x = \frac{M^3}{Z^2}\lambda\gamma_x,\ [0020]_y = \frac{M^3}{Z^2}\varepsilon\gamma_y,$$
$$[0002]_y = \frac{M^3}{Z^2}\lambda\gamma_y,\ [0002]_x = \frac{M^3}{Z^2}\varepsilon\gamma_x, \tag{1}$$
$$[0011]_x = \frac{M^3}{Z^2}\eta\gamma_y,\ [0011]_y = \frac{M^3}{Z^2}\eta\gamma_x,$$

where

M — linear magnification of the lens,

$Z = z_a - z_i$ — length of the region restricted by the aperture plane and the image Gaussian plane,

γ_x, γ_y — ideal deflection of the electron beam in DD.

The coefficients λ, ε, and η in the formulae (1) depend upon the magnetic field shape in the deflecting coils DD:

$$\lambda = \tfrac{3}{2}h_1 + Q,$$
$$\varepsilon = -\tfrac{1}{2}h_1 + Q,$$
$$\eta = rp_1 - p_2 + 2Q. \tag{2}$$

The coefficient h_1 is connected with linear properties of the deflecting-focusing unit [2]:

$$h_1 = p_2 - L - r(p_1 - L_1),$$

the significance of the symbols L, L_1, L_2 and p_1, p_2 being explained in fig. 1 [1]. The constant Q in the formula (2) depends upon the properties of the deflecting

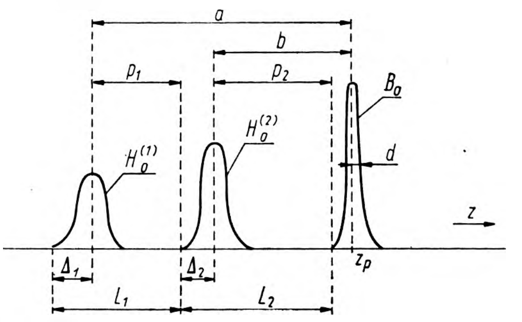

Fig. 1. The fields distribution along the electronooptical axis z, $H_0^{(1)}, H_0^{(2)}$ — deflecting field strengths in the first and second deflecting unit, B_0 — magnetic induction in the lens

field in DD coils. The deflecting field, e.g. a horizontal one, for the deflecting coils adjacent to the magnetic coat of the lens is [3]:

$$H_0(z) = NI\cos\Theta e(z),$$
$$H_2(z) = NI[\cos\Theta f(z) + \cos 3\Theta g(z)],$$

where

$$e(z) = -\frac{4}{\pi^2 R}\int_0^\infty \frac{\sin\frac{kl}{R}\cos\frac{kz}{R}}{I_1(k)}\,dk,$$
$$f(z) = -\frac{1}{2\pi^2 R^3}\int_0^\infty \frac{k^2\sin\frac{kl}{R}\cos\frac{kz}{R}}{I_2(k)}\,dk, \tag{3}$$
$$g(z) = -\frac{1}{\pi^2 R^3}\int_0^\infty \frac{k^2\sin\frac{kl}{R}\cos\frac{kz}{R}}{I_3(k)}\,dk.$$

NI — number of ampertums in deflecting coils,

$2l$ — length of the deflecting unit,

* Institute of Electron Technology of Wrocław Technical University Wrocław, Poland.

$D = 2R$ — diameter of the aperture in the end lens coat.

In this case the constant Q:

$$Q = r\left\{\Delta_1(\Delta_1^2+3\langle z_f^2\rangle_1)\frac{f_0^{(1)}}{e_0^{(1)}}+\Delta_1(\Delta_1^2+3\langle z_g^2\rangle_1)\times\frac{g_0^{(1)}\tilde{\Theta}_1}{e_0^{(1)}}\right\}-\Delta_2(\Delta_2^2+3\langle z_f^2\rangle_2)\frac{f_0^{(2)}}{e_0^{(2)}}-\Delta_2(\Delta_2^2+3\langle z_g^2\rangle_2)\frac{g_0^{(2)}\tilde{\Theta}_2}{e_0^{(2)}} \quad (4)$$

depends upon the zero and second moment of the function $e^{(i)}(z), f^{(i)}(z), g^{(i)}(z)$ and upon the field angle $\Theta_i (i = 1,2)$ of the deflecting coils (fig. 2).

$$e_0^{(i)} = 2\int_0^{\Delta_i} e^{(i)}(z)dz,\quad f_0^{(i)} = 2\int_0^{\Delta_i} f^{(i)}(z)dz,$$

$$g_0^{(i)} = 2\int_0^{\Delta_i} g^{(i)}(z)dz,$$

$$\langle z_f^2\rangle_i = 2\int_0^{\Delta_i} z^2\frac{f^{(i)}(z)dz}{f_0^{(i)}}, \quad (5)$$

$$\langle z_g^2\rangle_i = \int_0^{\Delta_i} z^2\frac{g^{(i)}(z)dz}{g_0^{(i)}}.$$

$$\tilde{\Theta}_i = 4\cos^2\Theta_i - 3.$$

The quality $\Delta_i (i = 1,2)$ used in eqs. (4) and (5) denotes the width of the deflecting field in the first or second deflecting system (comp. fig. 1). In our considerations the width of the deflecting field Δ_i has been assumed to be equal to ordinate for which the abscissa is 20 times smaller than the maximal value of the function $e^{(i)}(z)$,

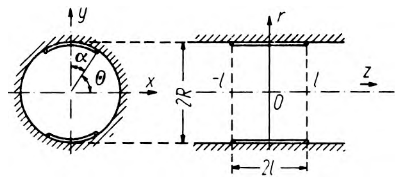

Fig. 2. Horizontal deflection unit

$$\Delta_i = (e^{(i)})^{-1}\left[\frac{e^{(i)}(0)}{20}\right],$$

where e^{-1} denotes the reverse function to $e(z)$. Also half-width of the magnetic induction B_0 in the lens has been assumed to be small as compared to the deflecting field widths Δ_1 and Δ_2. The zero and second moments of the functions $e(z), f(z)$, and $g(z)$ have been determined from the formulae (3) and (5) for the deflecting coils of lengths $2l = 20, 25, 30, 35$ and 40 mm given in table 1.

The condition of the proper action of DD has the form [1]:

$$\frac{a}{b} = n\frac{\cos\Theta_2}{\cos\Theta_1}\frac{e_0^{(2)}}{e_0^{(1)}},\quad n = \frac{N_2}{N_1} \quad (6)$$

where:

N_1 — winding number in the coils of the first deflecting unit,

N_2 — winding number in the coils of the second deflecting unit,

Θ_1, Θ_2 — field angles of the first and second deflecting units (see fig. 2).

While the following approximate relation holds (comp. fig. 1):

$$a \simeq L-\Delta_1,\quad b \simeq L_2-\Delta_2. \quad (7)$$

The semiaxes of the shifted coma and anticoma ellipse of DD depend upon the aperture angle ω, linear magnification M of the lens and the distance R_i of the Gaussian image of a point from the electronooptic axis in the working plane, the length L of the deflecting doublet DD and the coefficients λ, ε, and η [2]:

— the long semiaxis

$$R_i|K_1|\,M^2\omega^2,$$

— the short semiaxis

$$R_i|K_2|\,M^2\omega^2,$$

Table 1

The values of zero and second order moments for the functions $e(z)$, $f(z)$ and $g(z)$

l [m]	0.01	0.0125	0.015	0.0175	0.02
Δ [m]	0.04	0.042	0.043	0.045	0.0465
$-e_0$	0.8486	1.0605	1.2723	1.4837	1.6949
$-f_0 \cdot 10^2$	0.0258	0.0368	0.0515	0.0712	0.0977
$-g_0 \cdot 10^2$	60.2567	75.3152	90.3695	105.4184	120.4603
$\langle z_f^2\rangle \cdot 10^{-2}$	7.7531	6.7322	5.7160	4.7526	3.8791
$\langle z_g^2\rangle \cdot 10^{-4}$	2.0402	2.2156	2.4299	2.6830	2.9746

— the distance of the ellipse centre from the ideal imaging

$$R_l |K_3| M^2 \omega^2.$$

The coefficients derived below are called the coma parameters:

— parameter K_1 (connected with the long semiaxis)

$$K_1 = \frac{h_1}{L}, \tag{8a}$$

— parameter K_2 (connected with the short semiaxis)

$$K_2 = \frac{rp_1 - p_2}{2L} + \frac{Q}{L}, \tag{8b}$$

— parameter of asymmetry K_3

$$K_3 = \frac{h_1}{2L} + \frac{Q}{L}. \tag{8c}$$

The influence of the field angle of the deflecting coils on the parameters K_1, K_2 and K_3 are discussed in section 2. In the following section the influence of the deflecting-focusing unit sizes (section 3), and that of deflecting coils length (section 4) has been examined. The qualitative verification of the results obtained has been given in section 5.

2. The influence of the field angle Θ of deflecting coils on the deflection coma and anticoma of DD

It has been assumed that deflecting coils DD have equal dimensions, i.e.

$$l_1 = l_2 = l, \quad \Theta_1 = \Theta_2 = \Theta,$$

and also that the lengths L_1, L_2 for both the deflecting units are the least, i.e.

$$L_1 = 2\Delta_1, \; L_2 = 2\Delta_2$$

(comp. fig. 1 and [2]).

Five variants of the deflecting coils of lengths amounting to 20, 25, 30, 35 and 40 mm have been discussed. On the basis of relations (4) and (8) and the table 1 the parameters K_2 and K_3 may be represented in the form

$$K_{2,3} = -A_{2,3} \cos^2 \Theta_{2,3} + B_{2,3},$$

where the constants B_2, B_3 and A_2, A_3 depend upon the functions $e(z)$, $f(z)$ and $g(z)$. Hence, the field angle $\Theta_{2,3}$ of the coils, for which the parameters K_2 and K_3 disappear, amounts to

$$\Theta^*_{2,3} = \arccos \sqrt{\frac{B_{2,3}}{A_{2,3}}}. \tag{9}$$

The values of angles Θ^* for the variants mentioned above are presented in table 2, whereas, the graphs of parameters K_2 and K_3 for variants 1, 2 and 3 are given in fig. 3, as functions of the angle Θ. The graphs of parameters for the other variants (2,4) are positioned between the curves for variants 1 and 5. From fig. 3 and the analysis carried out it may be concluded that:

Table 2

The values of the angle Θ^* for which $K_2 = K_3 = 0$

Variant number	θ_2^*	θ_3^*
1	29.92°	29.97°
2	29.93°	29.98°
3	29.94°	29.98°
4	29.95°	29.99°
5	29.94°	29.99°

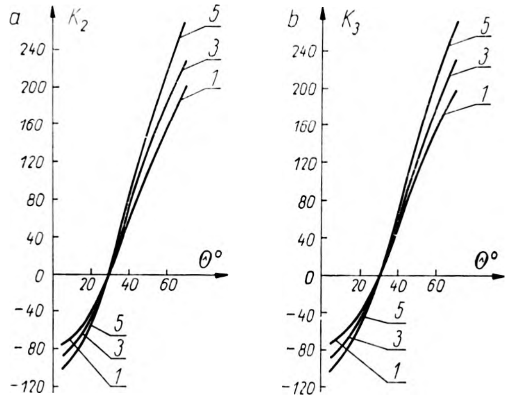

Fig. 3. The parameters K_2 and K_3 as a function of the angle Θ. a) K_2 versus Θ, b) K_3 versus Θ

— the parameters K_2 and K_3 are the least for an angle $\Theta \simeq 30°$ (comp. table 2).

— the increase of angle Θ causes quick increase of coma asymmetry parameter K_3 and parameter K_2,

— the increase of deflecting coils length $2l$ for an angle Θ different from 30° causes an increment of parameters K_2 and K_3,

— the parameter K_1 does not depend on the angle Θ.

3. The influence of deflecting focusing unit sizes on the deflection coma and anticoma

The quantities a and b (comp. fig. 4) are determined by the sizes of the deflecting-focusing unit (along the electronooptic axis z). It is convenient to introduce the quality $x = a-b$, which defines the distance

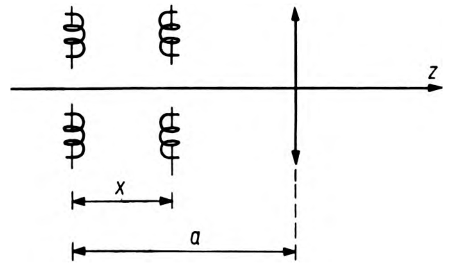

Fig. 4. The deflecting-focusing unit

between the deflecting units. When analysing the influence of a and x on the deflection coma and anticoma of DD it has been assumed that the field angles of both deflecting units are always the same and amount to

$$\Theta = 30^\circ.$$

This value of Θ has been chose since then

— the parameters K_2 and K_3 are small, as it follows from the analysis in section 2,

— the function $H_2(z)$ (comp. [3]) is similar to the curve (determined theoretically by Kaashoek [4]) assuring the least errors of the third order deflection of the deflecting units.

By virtue of the relation (8a) the parameter K_2 is proportional to the distance x between the deflecting units

$$K_1 = \frac{x}{a}. \tag{10a}$$

The dependence connecting the parameters K_2 and K_3 with the variable x has the form

$$K_{2,3} = p_{2,3}x^3 = q_{2,3}x^2+s_{2,3}x+t_{2,3}, \tag{10b}$$

where the constants $p_{2,3}, q_{2,3}, s_{2,3}$ and $t_{2,3}$ are

$$p_2 = p_3 = -\frac{1}{L}\frac{f_0^{(2)}}{e_0^{(2)}},$$

$$q_2 = -\frac{1}{L}\left(3\Delta_1\frac{f_0^{(2)}}{e_0^{(2)}}+\frac{a}{2}\right),$$

$$s_2 = -\frac{1}{L}\left(\frac{q_1}{a}+3\Delta_1^2\frac{f_0^{(2)}}{e_0^{(2)}}+3\langle z^2\rangle_2\frac{f_0^{(2)}}{e_0^{(2)}}-\frac{\Delta_2}{2a}-1\right),$$

$$t_2 = -\frac{1}{L}\left(\frac{a+\Delta_2}{2}+\Delta_1^3 f_0^{(2)}+3\Delta_1\langle z^2\rangle_2\times \times\frac{f_0^{(2)}}{e_0^{(2)}}-q_1\right), \tag{11}$$

$$q_1 = (\Delta_1^2+3\langle z^2\rangle_1)\Delta_1\frac{f_0^{(1)}}{e_0^{(1)}}, \langle z^2\rangle = \langle z_f^2\rangle,$$

$$q_3 = -3\Delta_1\frac{f_0^{(2)}}{e_0^{(2)}},$$

$$s_3 = -\left(\frac{1}{2a}+\frac{q_1}{aL}+3(\Delta_1^2+\langle z^2\rangle_2)\frac{f_0^{(2)}}{Le_0^{(2)}}\right),$$

$$t_3 = -\left(\Delta_1(\Delta_1^2+3\langle z^2\rangle_2)\frac{f_0^{(2)}}{e_0^{(2)}L}-\frac{q_1}{L}\right).$$

The graphs of parameters K_2 and K_3 as a function of x for $a = 150$, 200, 258 and 300 mm are presented in fig. 5. The graphs shown have been determined for $l_1 = l_2 = l$, and for deflecting coils of lengths 20, 25, 30, 35 and 40 mm. From fig. 5 it follows that:

— the increment of length a of the deflecting-focusing unit causes a decrease of K_2, while the increase of distance x between the deflecting units results in increment of K_2;

— the increment of deflecting unit length $2l$ causes the decrement of K_2;

— the increment of length a causes a shift of the intersection points of the set of K_2 functions with the x-axis toward the positive direction of the latter;

— at small values of the length a the increase of the length $2l$ of deflecting coils causes a decrement of K_3, while at great values of a an increase of the length $2l$ results in an increase of values K_3 (in the negative direction);

— the increase of the distance x between the deflecting units results in the decrease of K_3.

The asymmetry parameter of coma and anticoma K_3 causes a disturbance in symmetry of current density distribution in the transversal cross-section of the beam. Therefore, the sizes of the deflecting-focusing unit have to be selected so that the condition $K_3 = 0$ be satisfied. For coils of the same length ($l_1 = l_2$) is fulfilled this condition, if the distance between the deflecting units is:

$$\frac{-q_3\pm\sqrt{\delta}}{2p_3}, \tag{12}$$

where $\delta = q_3^2-4ps_3$, and the calculated distance between the deflecting units satisfies the inequality $2\Delta \leqslant x \leqslant a-\Delta$.

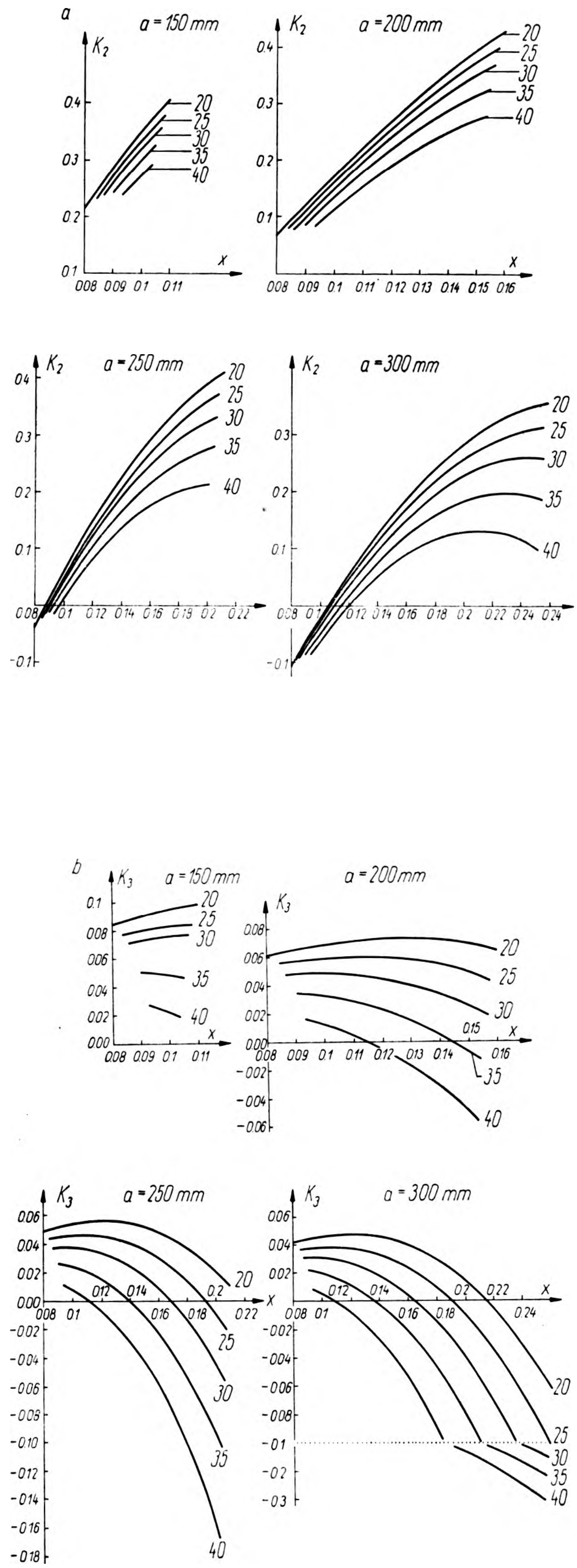

Fig. 5. The graphs of parameters K_2 and K_3 versus x: a) graph of K_2 versus x; b) graph of K_3 versus x; for $a = 150$, 200, 250 and 300 mm

4. The influence of the deflecting coil length on deflection coma and anticoma of DD

The dependence of the parameters K_1 and K_2 on the length of deflecting coils has been partially explained in the previous sections. In those sections the case $l_1 = l_2 = l$ has been discussed.

When analysing the influence of deflecting coil length on the coma it has been assumed (as in section 3) that

$$L_1 = 2\Delta_1, L_2 = 2\Delta_2, \Theta_1 = \Theta_2 = 30°.$$

The parameters K_1, K_2 and K_3 calculated from the formulae (11) are given in table 3. From these data the following conclusions may be formulated:

Table 3

The values parameters K_1, K_2 and K_3 versus the deflecting coils length

Parameters	l_2 \ l_1	0.01	0.0125	0.015	0.0175	0.02
K_1	0.01	0.6666	0.6721	0.6748	0.6800	0.6837
	0.0125	0.6619	0.6666	0.6692	0.6744	0.6781
	0.015	0.6586	0.6640	0.6666	0.6717	0.6754
	0.0175	0.6538	0.6590	0.6616	0.6666	0.6773
	0.02	0.6507	0.6555	0.6580	0.6630	0.6666
K_2	0.01	0.2906	0.2975	0.3020	0.3088	0.3159
	0.0125	0.2765	0.2824	0.2870	0.2928	0.2989
	0.015	0.2623	0.2677	0.2712	0.2774	0.2837
	0.0175	0.2411	0.2414	0.2494	0.2500	0.2596
	0.02	0.2161	0.2154	0.2187	0.2225	0.2328
K_3	0.01	0.0406	0.0414	0.0429	0.0441	0.0471
	0.0125	0.0326	0.0324	0.0340	0.0342	0.0362
	0.015	0.0214	0.0207	0.0212	0.0217	0.0239
	0.0175	0.0580	0.0006	0.0500	0.0000	0.0055
	0.02	−0.0156	−0.0219	−0.0215	−0.0234	−0.0172

— the increase of the length $2l_2$, for $2l_1 = \text{const}$, causes a decrease of K_1, while the increase of $2l_1$, for $2l_2 = \text{const}$, slightly increases K_1;

— if $l_1 = l_2$ then $K_1 = 0.6666$ independently of the coil length;

— the change of $2l_1$, for $2l_2 = \text{const}$, slightly affects the value of K_2 which increases with the increment of $2l_1$;

— the increase of $2l_2$, for $2l_1 = \text{const}$, causes the decrement of K_2;

— the change in $2l_1$, for $2l_2 = \text{const}$, slightly affects the value of K_3, while the increase of $2l_2$, for $2l_1 = \text{const}$, leads to decrement of K_3.

5. Verification of the results

The aberration figures of the deflecting-focusing unit have been observed in a specially made electron-beam lamp of Ø 500 mm diameter, and 540 mm length [5]. The figures obtained on the lamp screen are distorted by all kinds of aberrations of even order and by asymmetry aberrations. Nevertheless, by analysing the figures for different aperture angles the dominating geometrical aberrations may be distinguished.

First of all three variants of deflecting-focusing unit have been examined which has been presented sche-

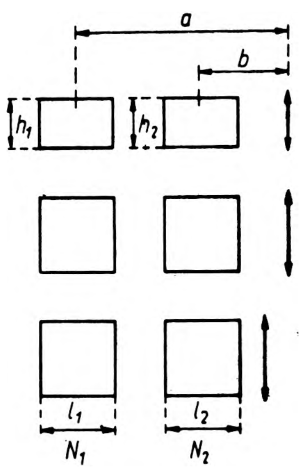

Fig. 6. The variants of the deflecting-focusing system

matically in fig. 6. For the three mentioned variants the deflecting coil sizes, i.e.: the length $2l$ and width h, as well as the distance a of the first deflecting system from the lens slit and the distance B of the second deflecting unit from the slit (see fig. 6) are given in table 4. In this table the ampertums of the deflecting coils DD is also given. The turn numbers N_1 and N_2 of the first and the second units respectively, are chosen in such a way that condition (6) be satisfied. Table 4 contains also two next variants which are discussed in detail in the further part of the section. In fig. 7 the aberration figures are presented for deviations (in the screen plane) along the x and y axis, equal to 3, 5, 8 mm in variants 1 and 3, and 3, 5 mm in variant 2, and for the aperture angles $\omega = 3°20'$, $4°10'$. The results obtained confirm the conclusion that at the increasing angle Θ the coma and anticoma decrease and the errors are least for coil field angle $\Theta = 30°$ (comp. fig. 8). The variant 3, compared to variant 2, introduces greater deviation coma and anticoma, thus confirming the conclusion obtained in section 3. In variants 4 and 5 the field angles of the

Table 4

The sizes of the deflecting-focusing unit in mms

Variant number	a	b	$2l_1$	h_1	$2l_2$	h_2	N_1	N_2
1	150	90	35	20	35	20	50	83
2	150	90	35	35	35	35	50	83
3	120	60	35	35	35	35	40	80
4	135	45	35	62	35	62	25	75
5	124	42	20	62	25	62	32	76

deflecting coils amount to 30° which results in smaller aberrations compared with the first three variants. The aberration figures for both the variants for deflection 5, 8 and 10 mm are presented in fig. 8. The aberration figures of variant 4 and 3 for the aperture angles 3°20′ and 4°10′ and deflections 10, 15 mm are shown, additionally, in fig. 9. The variant 4, is accordance with the table 3, has the least asymmetry parameter K_3. The aberration figures for variants 4 and 5 with switched-out lens of the deflecting-focusing unit are shown in fig. 10 for the aperture angle $\omega = 1°50', 3°20', 4°10', 5°21'$. The figures at the points of coordinates 10×10 mm, and at points 15×15 mm are presented in fig. 10a and 10b, respectively. A greater symmetry of the aberration figure seen for the fifth variant is evoked by a higher value of parameter K_3.

6. Concluding remarks

The above analysis of deflection coma and anticoma of DD includes only one type aberration. The analysis of the other eleven aberrations has been given in the paper [2]. The problem of optimizing the deflecting-focusing unit with respect to minimum coma is very important because this kind of aberrations can not be dynamically compensated [6]. As a result of analysis of deflection coma and anticoma it has been stated that:

— the increase of the distance between the deflecting systems causes an increase of coma and anticoma,

— the coma and anticoma diminish with the increase of deflecting coil length of DD, while the influence of the changes in the coil length of the first deflecting system is small as compared with the influence of the second system,

— the increase of the deflecting-focusing unit length diminishes the coma and anticoma.

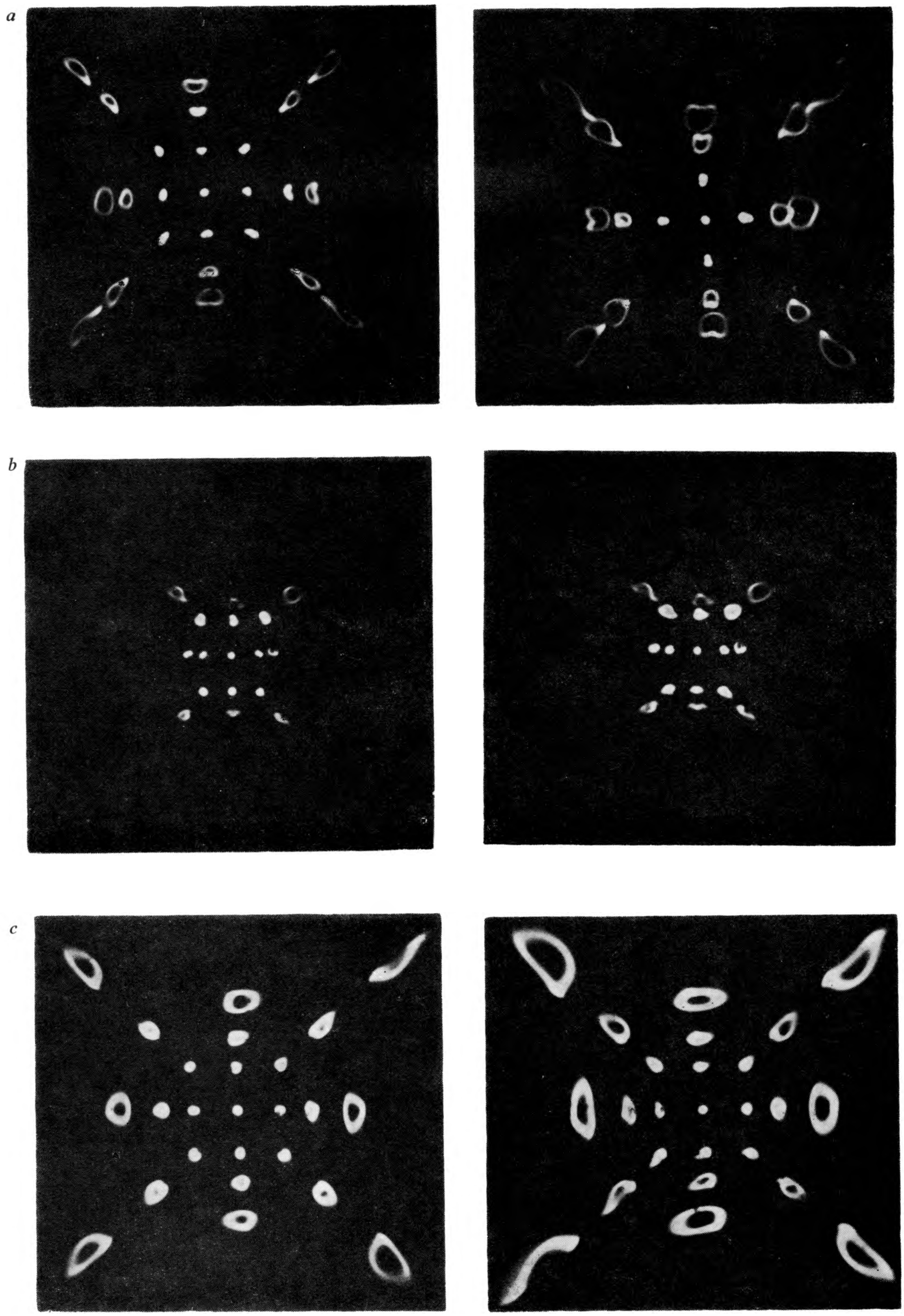

Fig. 7. The aberration figures for the aperture angles $\omega = 3°20'$, $4°10'$
a) variant 1 — deflection 3, 5, 8 mm; b) variant 2 — deflection 3 and 5 mm; c) variant 3 — deflection 3, 5 and 8 mm

a

b

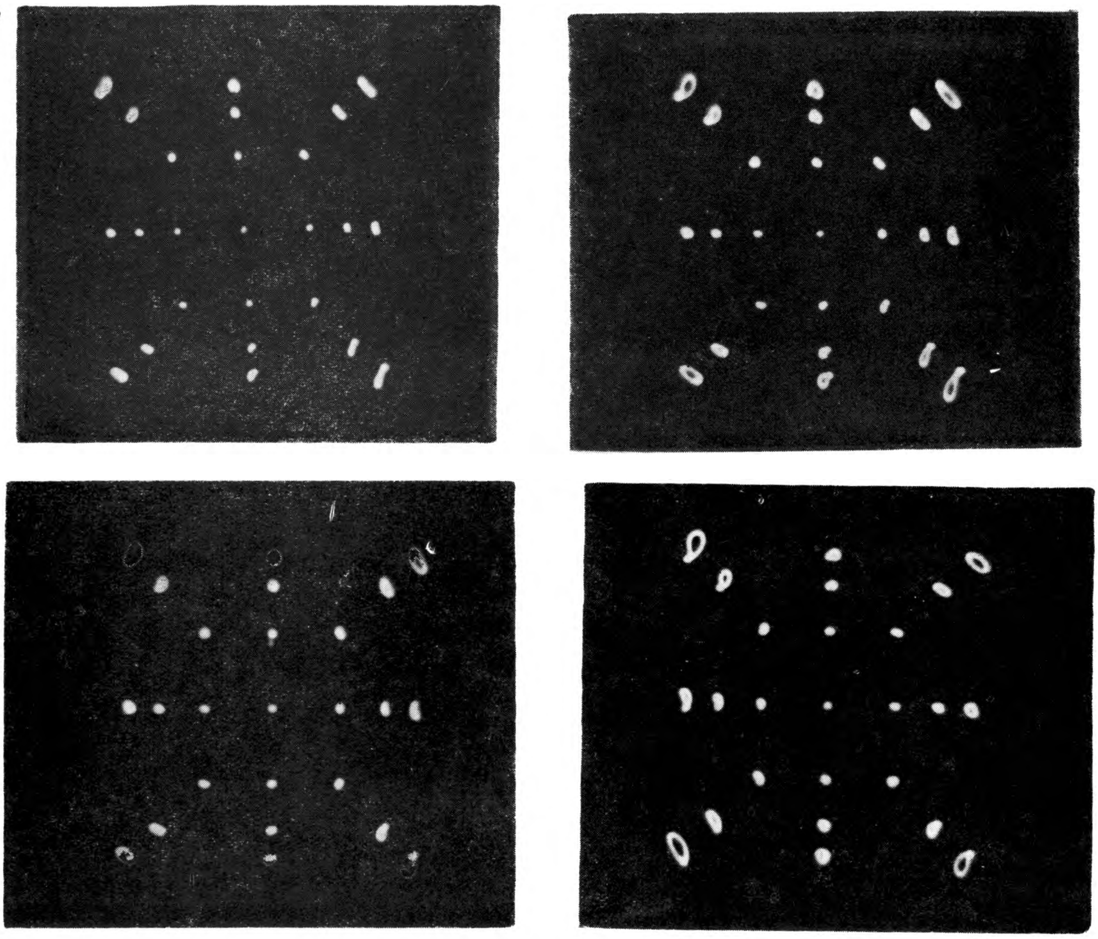

Fig. 8. The aberration figures for the aperture angle $\omega = 3°20', 4°10'$; deflection — 5, 8 and 10 mm; a) variant 4, b) variant 5

a

b

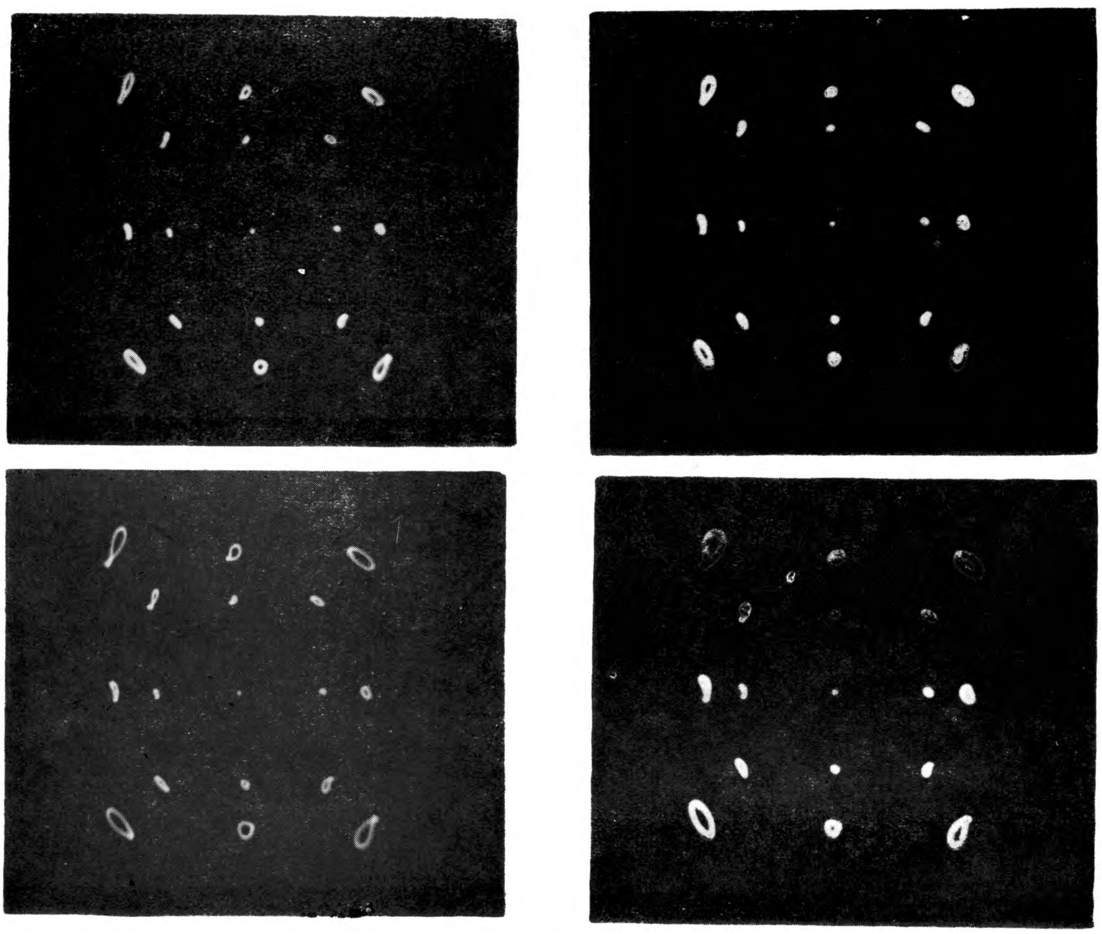

Fig. 9. The aberration figures for the aperture angles $\omega = 3°20', 4°10'$; deflection — 10 and 15 mm; a) variant 4, b) variant 5

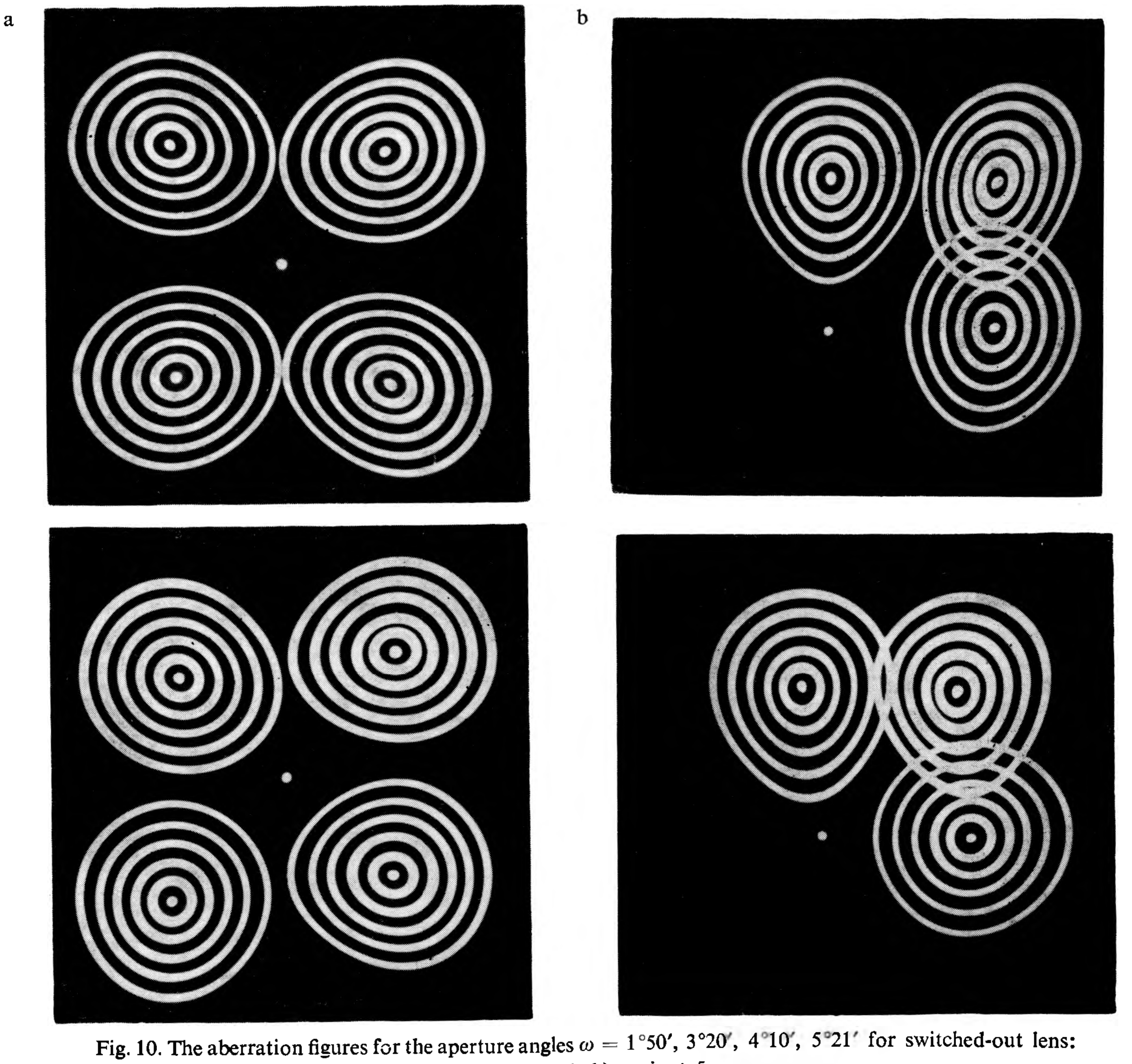

Fig. 10. The aberration figures for the aperture angles $\omega = 1°50', 3°20', 4°10', 5°21'$ for switched-out lens: a) variant 4, b) variant 5

The results obtained are confirmed by aberration figures observed on the screen for five different variants of the deviating-focusing unit.

Acknowledgements

The author expresses his thanks to Doc. Dr. Andrzej Mulak for his helpful remarks in formulation of the paper.

Кома и антикома отклоняюще-фокусирующей системы растрового микроскопа

Обсуждены кома и антикома отклонения растрового микроскопа. В анализе учитываются влияние размеров седлообразных отклоняющих катушек и размеры отклоняюще-фокусирующей системы. Полученные результаты проверены опытным путем.

References

[1] Romanowski A., *The linear approximation for the deflecting of the scanning microscope*, Optica Applicata VI, 3, 93–97 (1976).

[2] Romanowski A., *Third order aberrations of the electron deflecting-focusing system*, Optica Applicata VII, 4 (1977).

[3] Romanowski A., *Magnetic field in deviating coils of the analysing microscope*, Optica Applicata VI, 2, 35–38 (1976).

[4] Kaashoek I., *A study of magnetic-deflection errors*, Philips Res. Rep. Suppl., 11, 1–113 (1968).

[5] Romanowski A., *Podwójny układ odchylający z uwzględnieniem aberracji geometrycznych trzeciego rzędu*, Pr. nauk ITE PWr., nr 14, seria: Konferencje nr 2, 43–49, Wrocław 1975.

[6] Owen G., Nixon W. C., *Aberration correction for increased lines per field in scanning electron beam technology*, J. Vac. Sci. Technol. **10**, 6, 983–986 (1973).

Received, July 15, 1977